



Contents lists available at ScienceDirect

Tectonophysics

journal homepage: www.elsevier.com/locate/tecto

Faulting characteristics of supershear earthquakes

Michel Bouchon ^{a,*}, Hayrullah Karabulut ^b, Marie-Paule Bouin ^c, Jean Schmittbuhl ^d, Martin Vallée ^e,
Ralph Archuleta ^f, Shamita Das ^g, François Renard ^a, David Marsan ^h

^a Centre National de la Recherche Scientifique and Université Joseph Fourier, Grenoble, France

^b Kandilli Observatory and Earthquake Research Institute, Istanbul, Turkey

^c Observatoire Volcanologique de Guadeloupe, Guadeloupe, France

^d Centre National de la Recherche Scientifique and Université de Strasbourg, Strasbourg, France

^e Géosciences Azur, Université de Nice, Nice, France

^f Department of Earth Science, University of California, Santa Barbara, CA, United States

^g Department of Earth Sciences, University of Oxford, Oxford, UK

^h Université de Savoie, Chambéry, France

ARTICLE INFO

Article history:

Received 21 October 2009

Received in revised form 7 June 2010

Accepted 16 June 2010

Available online xxxx

Keywords:

Earthquake rupture

Rupture velocity

Fault geometry

Earthquake dynamics

Supershear rupture

ABSTRACT

Recent observations of large continental strike-slip earthquakes show that different fault segments may rupture at different speeds and that rupture may propagate faster than the shear wave velocity of surrounding rocks. We report that all the documented occurrences of supershear rupture are associated with faults which have simple geometry. The surface trace of these faults is described in the field or seen on satellite images as remarkably linear, continuous and narrow. Segmentation features along these segments are small or absent and the deformation is highly localized. As theoretically predicted, supershear is clearly associated with Mode II rupture.

© 2010 Elsevier B.V. All rights reserved.

1. Introduction

Rupture of a material can be described as a combination of three modes. In Mode I the displacement discontinuity (slip) between the two faces of the crack is normal to the crack faces. In the other two modes, slip occurs along the surface of discontinuity, in the direction perpendicular to the crack front (Mode II) or in the direction parallel to it (Mode III). Earthquakes are a combination of Mode II and Mode III rupture. Mode III is prevalent in large subduction earthquakes while Mode II is predominantly the mode of rupture of long strike-slip faults. In Mode I, rupture speed cannot exceed the Rayleigh velocity of the material while the limiting speed for Mode III is the shear wave velocity. In the 1970s, theoretical studies in fracture dynamics (Burridge, 1973; Freund, 1979) and numerical studies (Andrews, 1976; Das and Aki, 1977) showed that Mode II rupture cannot propagate between the Rayleigh and the shear wave velocities but can propagate faster than the shear wave of the material and up to its P-wave speed.

These theoretical predictions have been confirmed by laboratory experiments (Rosakis et al., 1999; Xia et al., 2004). Indeed the first direct measurement of rupture velocity in a material was supershear (Rosakis et al., 1999).

The first inference of an earthquake rupture velocity exceeding the shear wave speed was made during a Mw 6.5 strike-slip earthquake in California, the 1979 Imperial Valley earthquake (Archuleta, 1984; Spudich and Cranswick, 1984). In the subsequent 20 years no other observation of supershear rupture was reported. A possibility to account for the Imperial Valley observation and the lack of further reports is that the 1979 earthquake was exceptionally well recorded. Studies of large strike-slip earthquakes which have occurred over the last decade, under improved recording conditions, have shown several occurrences of supershear rupture. Such observations have been reported for the Mw 7.6 1999 Izmit (Turkey) earthquake (Ellsworth and Celebi, 1999; Bouchon et al., 2000, 2001), the Mw 7.2 1999 Düzce (Turkey) earthquake (Bouchon et al., 2001; Bouin et al., 2004; Konca et al., 2010), the Mw 7.8 2001 Kunlun (Tibet) earthquake (Bouchon and Vallée, 2003; Robinson et al., 2006; Vallée et al., 2008; Walker and Shearer, 2009; Wen et al., 2009), the Mw 7.9 2002 Denali (Alaska) earthquake (Aagaard and Heaton, 2004; Dunham and Archuleta, 2004; Ellsworth et al., 2004; Frankel, 2004; Walker and Shearer, 2009). It seems well established that in each case, rupture propagated at varying velocity, reaching supershear speed on some fault segments while breaking others at sub-Rayleigh velocity.

What then characterizes supershear fault segments? To try to answer this question, we begin with what is the simplest and most obvious observable concerning a fault: its geometry.

* Corresponding author.

E-mail address: Miche.Bouchon@ujf-grenoble.fr (M. Bouchon).

2. Fault geometry

2.1. Imperial Valley earthquake

The surface faulting produced by the 1979 Imperial Valley earthquake was mapped in detail in the field by Sharp et al. (1982). The segment along which supershear rupture speed was inferred is shown in Fig. 1.

The surface expression of the fault over this section, a little over 5 km long, is a simple continuous linear scarp. As described by Sharp et al. (1982) “the surface ruptures [in this area] were generally restricted to a single echelon mole track”. This segment begins near an 85 m step-over in the rupture trace termed “the most notable of the complexities” of the southern half of the surface rupture (Sharp et al., 1982). The end of this segment corresponds to the junction of the Imperial fault with the

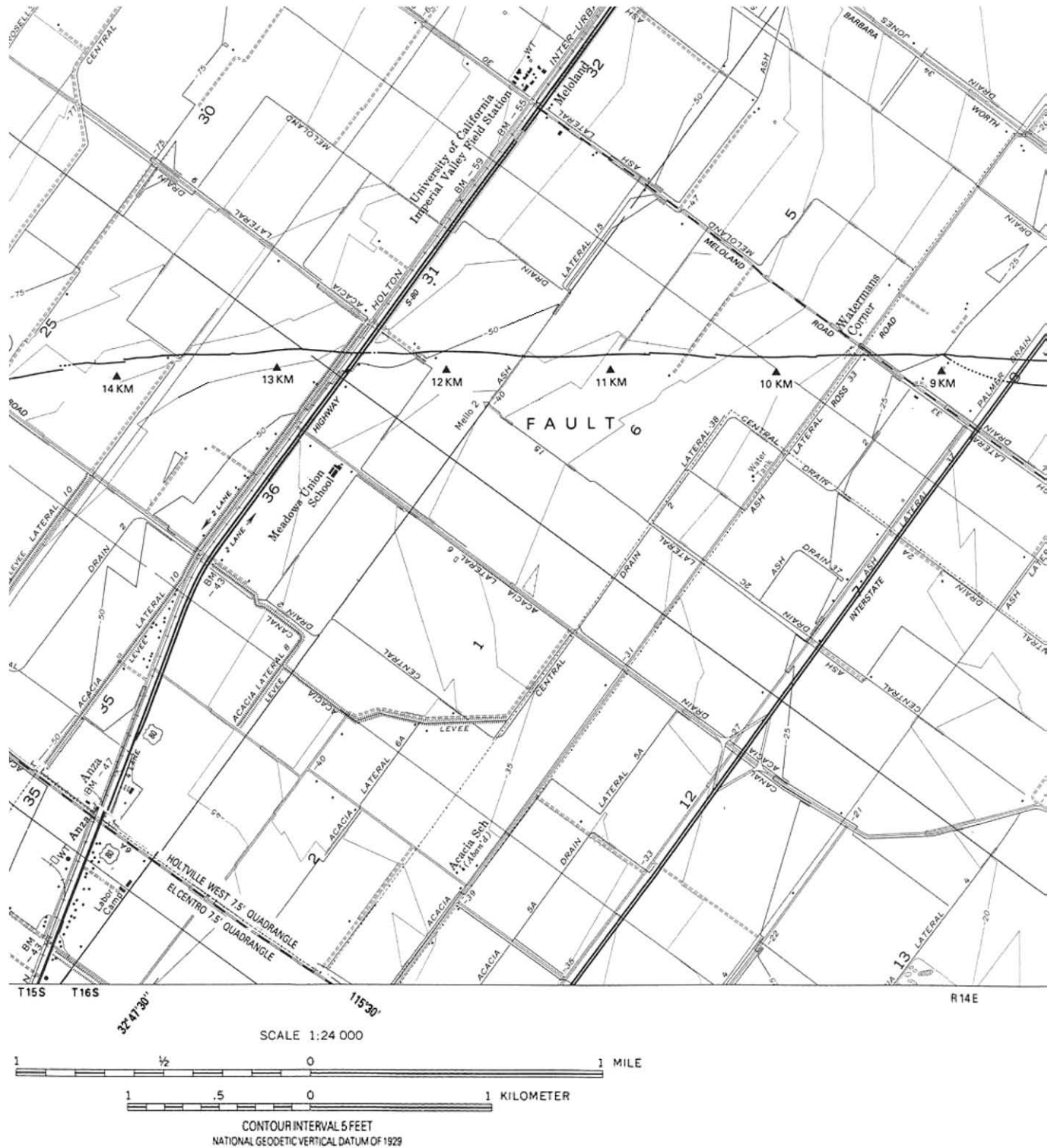
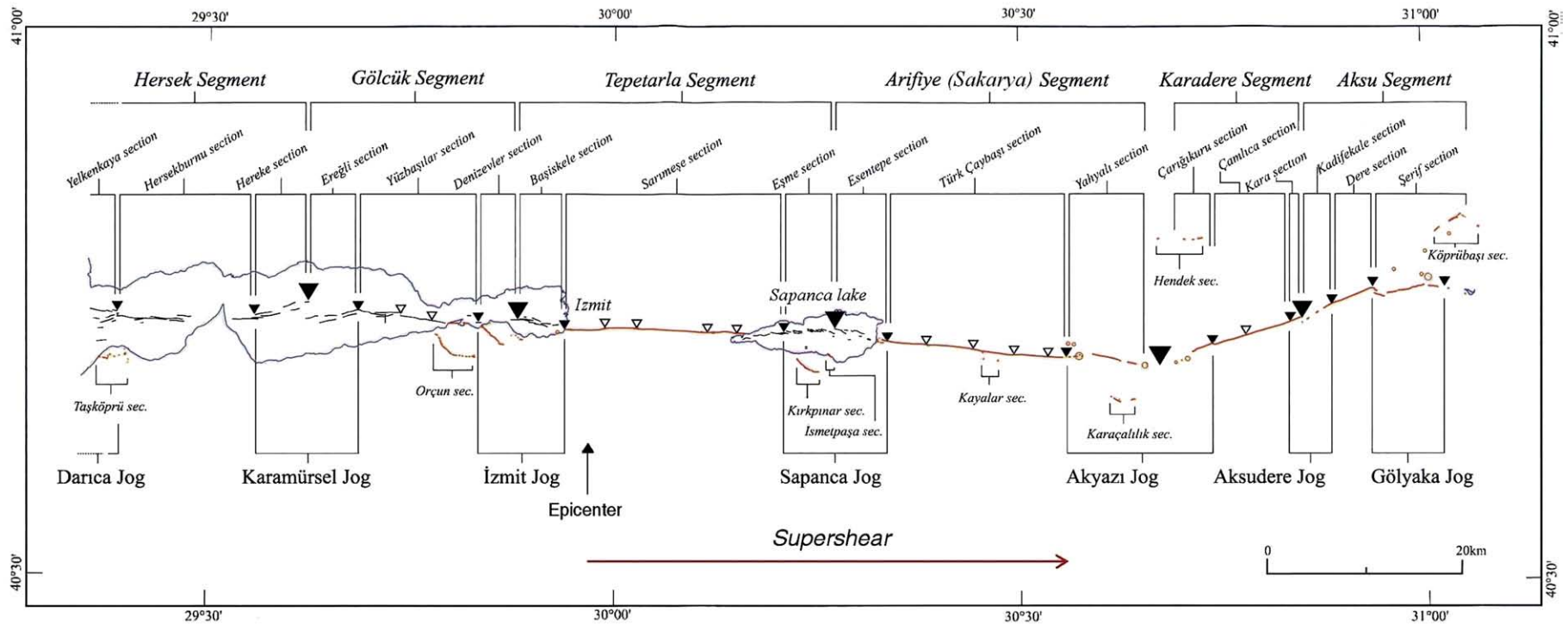


Fig. 1. Trace of the surface rupture produced by the Imperial Valley earthquake in the zone where supershear rupture was inferred by Archuleta (1984). Kilometric values along the fault trace indicate the distance from the start of the surface break. After Sharp et al. (1982).



Segment structure of the surface rupture of the August 17, 1999 İzmit earthquake

Fig. 2. Segmentation of the surface trace of the İzmit rupture. The red trace indicates the observed (on land) rupture. The black trace is the estimated (underwater) rupture. Solid triangles denote major segmentation features while small open triangles indicate small segmentation features. The epicenter and the extent of the supershear episode are shown. Modified from Awata et al. (2003).

Brawley fault where branching of the rupture occurred with both faults rupturing.

2.2. Izmit earthquake

The map of the surface trace of the Izmit rupture is shown in Fig. 2. This map displays the segmentation of the rupture inferred from field observations by Awata et al. (2003). The part of the fault on which supershear rupture was inferred extends eastward from the hypocenter for about 50 km. It includes the Izmit-to-Sapanca (also called Sarimese) section, the fault segment under Sapanca lake and most of the Sakarya (or Arifiye) segment. Along this supershear strand, the surface expression of the fault has been characterized by all the field investigators as simple, linear, and narrow: “Surface rupture [along the Izmit–Sapanca segment] indicates a narrow (0.5 to 3 m) deformation zone in general” (Barka et al., 2002); “The Sapanca–Akyazi segment is typically expressed as a narrow (2–8 m wide) rupture zone” (Barka et al., 2002); “Typically, the faulting [on the Sakarya fault segment] was confined to a simple trace, with little motion transferred to secondary fractures or spays. Surface deformation was expressed as a narrow zone of cracks” (Langridge et al., 2002); “The Sapanca segment is characterized by a relatively simple, narrow (1–5 m wide) straight fault trace” (Hartleb et al., 2002); “Surface rupture [along the Sakarya segment] is typically expressed as a narrow (2–8 m wide) fault zone” (Hartleb et al., 2002).

Satellite images of the ground deformation obtained by SPOT photograph correlation (Feigl et al., 2002; Michel and Avouac, 2002) show the “very linear discontinuity” (Michel and Avouac, 2002) of the ground displacement along the supershear fault strand (Fig. 3). These authors further emphasize that along this strand “the coseismic slip was entirely accommodated along the rupture seen at the surface” and that “there was little if any coseismic deformation taken up by distributed shear off the main fault’s trace” and they conclude that “the surface ruptures seem remarkably simple”.

Eastward of Sapanca lake, the Sakarya segment is linear and continuous for about 18 km. Then, the rupture abruptly makes a 1.5 km-wide step to the north (Barka et al., 2002; Langridge et al., 2002). This restraining step-over marks the end of the simple nearly-continuous linear surface break mapped in the field and imaged from space, which extends eastward for about 50 km from the epicentral area. Its location closely corresponds to the end of the inferred supershear episode of the rupture (Bouchon et al., 2002). However, the space–time model inferred for the rupture from the near-fault recordings is not precise enough to know if this step-over provoked the end of the supershear episode or if the rupture had already decelerated a few kilometers before.

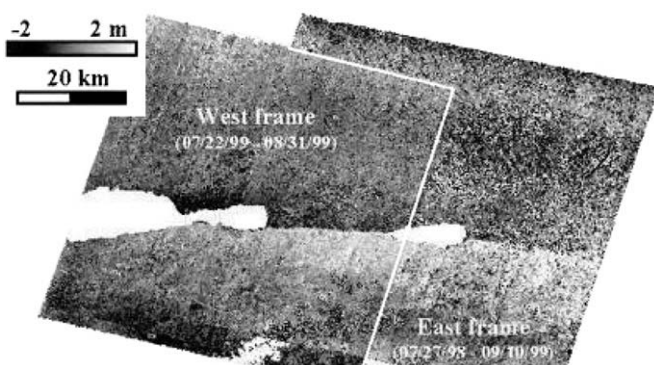


Fig. 3. Optical satellite image of the Izmit region obtained by correlating two sets of photographs (SPOT) taken before and after the earthquake. The image shows the strong and linear localization of the deformation along the supershear segment (see Fig. 2 for geographic referencing). After Michel and Avouac (2002).

Quite remarkably, the part of the fault where supershear rupture was inferred seems free of any significant geometric segmentation (Awata et al., 2003, Fig. 2), except, possibly, under Sapanca lake. The geometry of the fault under the lake, however, is not directly known. Some geologists have argued that the lake is a pull-apart basin (Barka et al., 2002; Lettis et al., 2002) and that the fault steps over from the Izmit–Sapanca segment, which they suggest runs near the northern margin of the lake, to the Sakarya segment, located one or two kilometers to the south. However, other authors are less affirmative about the existence of this step-over. For Aydin and Kalafat (2002), if “it is possible that there may be [a] discontinuity or step-over in the rupture zone under the lake”, “it is unlikely that the lake Sapanca step-over is as wide as the lake itself and is solely responsible for the present form of the lake.” They propose “that lake Sapanca [] owes its geometry and size to faults immediately to the north and south of the lake in addition to the fault strands associated with the Izmit earthquake”. Arpat et al. (2001) and Herece and Akay (2003) consider that the fault is continuous under the lake. The lake bathymetry (Lettis et al., 2002) does not show any direct evidence of a step-over between the Izmit–Sapanca segment to the west and the Sakarya segment to the east. Indeed, as can be seen in Figs. 2 or 3, the linear extrapolation of the Sakarya segment westward across the lake would meet the Izmit–Sapanca segment near the very location where it enters the lake. A set of observations which strongly argues against the presence of a step-over beneath the lake is the spatial slip distribution which shows that the zone of maximum slip occurred around Sapanca lake (Reilinger et al., 2000; Barka et al., 2002; Michel and Avouac, 2002; Awata et al., 2003; Çakir et al., 2003a). Such an observation seems difficult to conciliate with the fact that slip usually goes to a minimum at a step-over. As stated by Michel and Avouac (2002): “Unexpectedly, it seems that the near-fault slip tends to be maximum at the junction between the fault segments”. Thus, we believe that data and observations now available favor the geometric continuity of the fault under lake Sapanca.

2.3. Düzce earthquake

The Düzce earthquake occurred three months after the Izmit earthquake and extended the 150 km long rupture some 40 km eastward. Like the Izmit earthquake, it was a bilateral event nucleating near the middle of the fault (Fig. 4) and near-field recordings show some evidence that, while rupture propagated westward from the hypocenter at sub-Rayleigh velocity, the eastward propagation occurred at an average speed exceeding the crustal shear wave velocity (Bouchon et al., 2001; Bouin et al., 2004; Konca et al., 2010). Remarkably, this inferred difference in rupture speed corresponds to clearly marked differences in the rupture geometry and morphology: As described by Pucci et al. (2006), who made the most extensive field study of the Düzce rupture: “Overall, we recognized two different sections of the Düzce segment: a western section, where the coseismic fault trace has a staircase trajectory and reactivated part of the older fault system; an eastern section, where the coseismic fault trace shows a straight trajectory and cross-cuts the older and complex fault system”. These differences are detailed in Pucci (2006): “The present-day Düzce fault activity occurs along two fault sections that show different architecture: (1) the western section where the coseismic fault trace follows mainly the saw-tooth trajectory of the pre-existing regional fault system [], and (2) the eastern section, where the coseismic fault trace cross-cuts and violated completely the en-échelon pattern of the regional fault system”. As also noted by Akyüz et al. (2002), this eastern section of the fault is remarkably narrow and linear.

2.4. Kunlun earthquake

The Kunlun (also called Kokoxili) earthquake occurred along one of the major strike-slip faults of Tibet and produced the longest

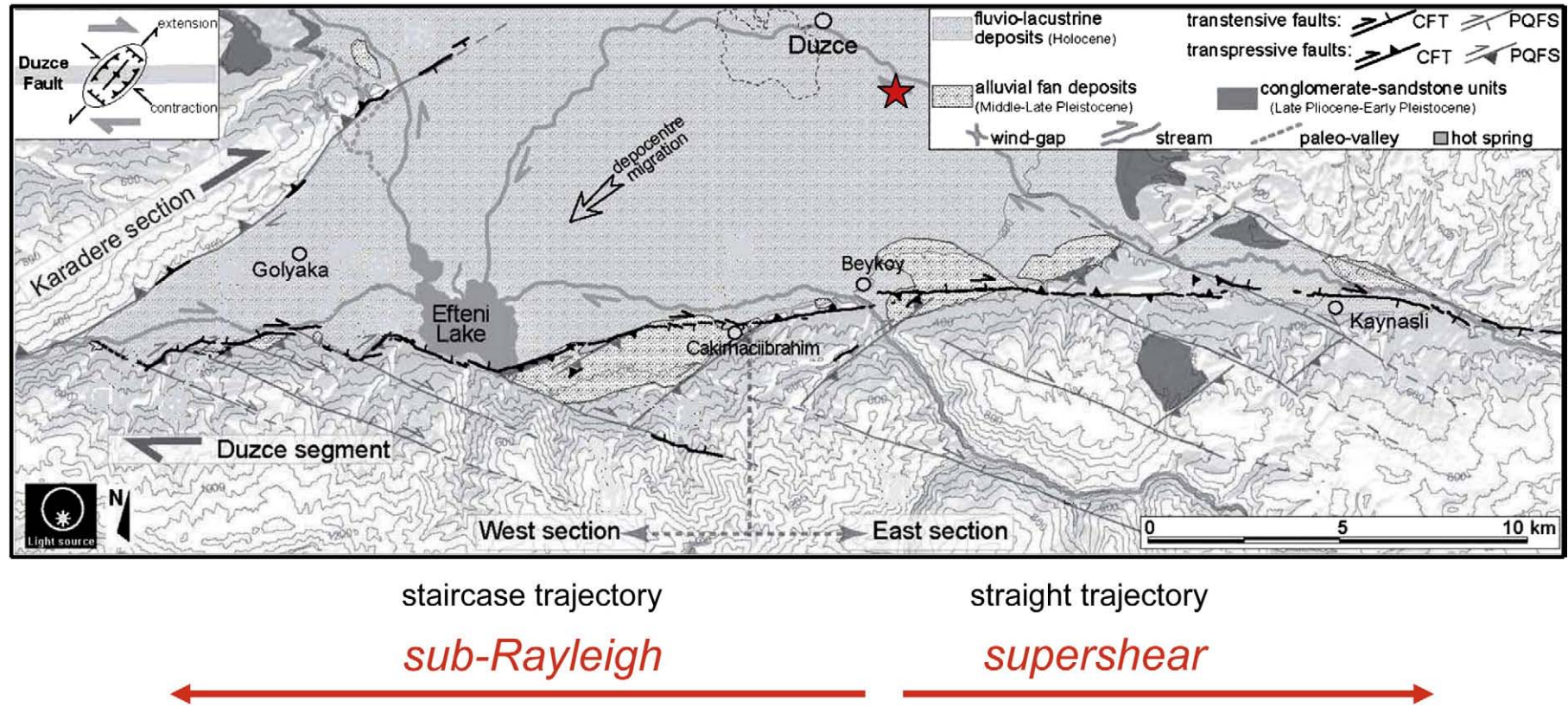


Fig. 4. Map of surface rupture of the Düzce earthquake (black line). The epicenter is shown by the star. The fault dips about 65° northward. The red arrows show the zones where sub-Rayleigh and supershear rupture velocities were inferred. Modified from Pucci (2006).

surface rupture ever observed, a nearly-continuous break extending for about 425 km (Xu et al., 2006) (Fig. 5). This surface rupture can be divided into three main sections displaying different structures and morphologies: In the west, where the earthquake began, a strike-slip section about 26 km long on a secondary fault which is part of the horsetail fault system that ends the Kunlun fault westward, followed by a 50 km long transtensional section and after a sudden bend of about 20° in strike, a remarkably straight 350 km long strike-slip section. Seismic records indicate that the first two sections broke at sub-Rayleigh velocity, but that some time after reaching the long and straight stretch of the Kunlun fault, rupture accelerated considerably, breaking most of this very long segment at supershear speed (Bouchon and Vallée, 2003; Robinson et al., 2006; Vallée et al., 2008; Walker and Shearer, 2009; Wen et al., 2009).

The surface rupture of this main segment has been mapped in great detail during several field investigations (Lin et al., 2002; van der Woerd et al., 2002; Xu et al., 2003, 2006; King et al., 2005) and using high-resolution satellite imagery (Fu and Lin, 2003; Fu et al., 2005; Klinger et al., 2005, 2006; Lasserre et al., 2005). The major characteristic of this 350 km long stretch of the fault, which comprises the Hongshui He/Kusai Hu segment (often simply referred to as the Kusai Hu segment) and the Kunlun Pass segment, is its straight geometry (Fig. 5). As described by van der Woerd et al. (2002), “The Kusai Hu segment of the Kunlun fault is remarkably straight between 91° and 94°”. As also noted by Klinger et al. (2006), “From the point where the ruptured joined the Kusai section, it propagated eastward for about 270 km without any major change in strike.” This linearity is particularly evident from space: “In the satellite image, the traces of the Kusai Lake and Kunlun Pass faults exhibit striking lineaments” Fu et al. (2005).

After rupturing the 270 km long Kusai Hu segment, rupture, instead of bending its path northward to continue on the main Kunlun fault, kept propagating nearly straight along a secondary strand, the Kunlun Pass fault, which lies in the direct prolongation of the Kusai segment.

2.5. Denali Fault earthquake

The Denali Fault earthquake ruptured the earth's surface over about 340 km along three different faults (Fig. 6). It initiated on a thrust fault and then propagated as a strike-slip rupture, first for about 220 km along the Denali fault, then for another 66 km along the

Totschunda fault. There is some evidence (Aagaard and Heaton, 2004; Dunham and Archuleta, 2004; Ellsworth et al., 2004; Frankel, 2004; Walker and Shearer, 2009) that after beginning at sub-Rayleigh velocity, rupture propagated at supershear speed over part of the Denali fault before decelerating again to sub-Rayleigh velocity. The precise length of the supershear segment is unknown. What seems well established is that rupture went by the only near-fault accelerometer station at supershear speed (Aagaard and Heaton, 2004; Dunham and Archuleta, 2004; Ellsworth et al., 2004). Modeling of the ground motion recorded there indicates that rupture had propagated at that speed for at least 35 km before reaching the station (Dunham and Archuleta, 2004). Details of the corresponding surface rupture over this relatively short range are sparse. It is “typically a single break, without splays or parallel traces” (Haeussler et al., 2004). A large part of it occurs in glacier ice where it is “usually expressed as a jogged linear trace [] influenced by the ice fabric” (Haeussler et al., 2004).

3. Surface slip characteristics

3.1. Imperial Valley earthquake

The modeling of the near-fault recordings shows that the largest slip during the 1979 earthquake—about 1.6 m—occurred on the short supershear section of the fault (Archuleta, 1984), and that it was nearly pure strike-slip. Only a small portion of this slip, about 40 cm, reached the surface, producing ground fracturing typical of strike-slip fault ruptures (Sharp et al., 1982). The vertical component of slip there was minor, in contrast to the fault section to the north where the vertical component of movement was relatively large and was often the dominant component (Sharp et al., 1982).

3.2. Izmit earthquake

The slip distribution along the surface rupture, obtained from field measurements, is displayed in Fig. 7 (Awata et al., 2003). Along the supershear segment, motion is almost purely right-lateral. When present, vertical displacement is considerably smaller. This explains the weak geomorphic expression of the fault along the Izmit–Sapanca segment and the non-recognition of the Sakarya fault segment prior to the earthquake (Emre et al., 1998; Langridge et al., 2002). The

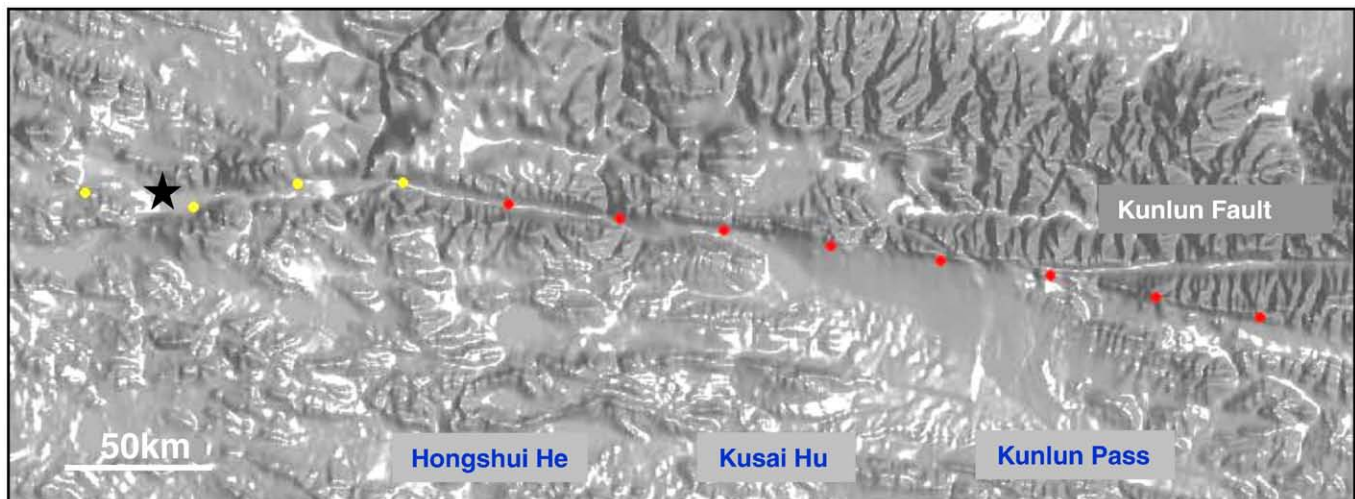


Fig. 5. Topographic image of the Kunlun earthquake region. The epicenter is indicated by a star. The rupture trace is shown by the dots. Yellow and red dots indicate respectively sub-Rayleigh and supershear rupture speeds.

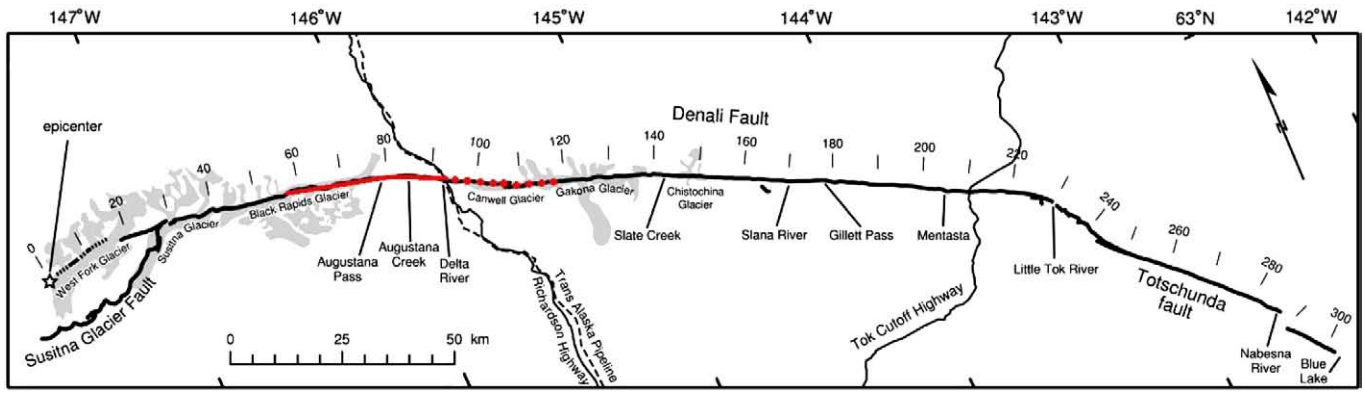


Fig. 6. Map of surface rupture of the Denali earthquake. The segment where supershear rupture was inferred by Ellsworth et al. (2004) and Dunham and Archuleta (2004) is shown by the red line. Continuation of the supershear segment eastward (red dots) from the lone near-fault accelerometric station, located along the Trans Alaska Pipeline, is uncertain. Modified from Haessler et al. (2004).

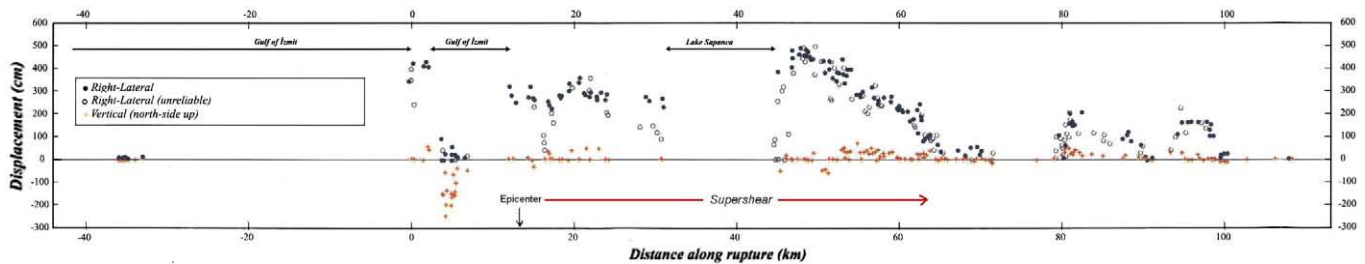


Fig. 7. Surface slip measured in the field along the Izmit rupture. The geographic extent of the supershear segment is indicated. Modified from Awata et al. (2003).

variation of slip along the 50 km long supershear rupture is also remarkably smooth.

3.3. Düzce earthquake

As described in the field (Aydin and Kalafat, 2002): “The surface faulting of the Düzce earthquake may be considered in three parts: the western and central parts are characterized by transtension and transpression respectively. The eastern part [where supershear was inferred] displays typical strike-slip faulting. The vertical component along this segment is minor and shows varying polarity”. The quasi-absence of vertical slip on the section of the fault where supershear occurred (Fig. 8) is surprising as the Düzce fault is an oblique fault plane dipping about 65° northward (Özalaybey et al., 2000; Bürgmann et al., 2002; Çakır et al., 2003b; Bouin et al., 2004; Konca et al., 2010). The correlation of satellite optical images (Konca et al., 2010) confirms that slip on the supershear segment is along strike and is smoothly varying. Thus, again with the Düzce earthquake, the supershear episode is associated with pure strike-slip faulting. Right-lateral slip on this segment stays around 3 m before sharply decreasing towards the end (Akyüz et al., 2002).

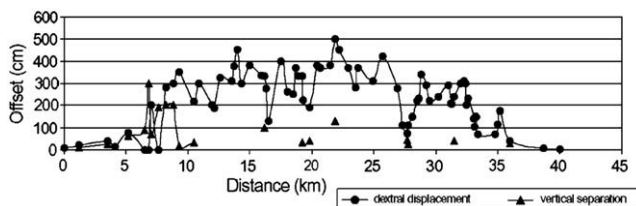


Fig. 8. Surface slip measured along the Düzce rupture. From Akyüz et al. (2002).

3.4. Kunlun earthquake

The first part of the long linear section of the Kunlun rupture—the 115 km long Hongshui He subsection—is “characterized by localized left-lateral faulting with only minor vertical motion” (Xu et al., 2006). There, as described by Klinger et al. (2005): “For over 100 km eastward, the 2001 rupture is mostly single stranded and exhibits nearly pure strike-slip motion.” To the east, this segment ends near the outlet of the Hongshui He river, at which location the rupture splits eastward in two subparallel segments (Klinger et al., 2005). For about 70 km, these two surface rupture traces coexist (Fig. 9). The nature of the two ruptures is remarkably different: “The southern strand that cuts through bajadas and fan surfaces exhibits almost pure strike-slip motion with typical associated morphology. The northern strand is located at the base of the Kunlun range front, about 2 km north from the southern strand, and exhibits mainly normal faulting with vertical motion in the range of 0.5 to 1 m” (Xu et al., 2006). This partitioning between coseismic strike-slip and normal faulting is remarkable (King et al., 2005; Klinger et al., 2005). Although the occurrence of dip-slip and strike-slip motion on parallel faults had been observed before, the Kunlun earthquake provides the first unequivocal demonstration that this partition of slip, localizing almost pure strike-slip and normal faulting on two parallel fault strands, may occur simultaneously during one single event (Klinger et al., 2005).

The fact that only Mode II ruptures—strike-slip motion in the present case—can propagate at supershear speed, while Mode III ruptures—the normal dip-slip motion in Kunlun—cannot exceed the shear wave velocity of surrounding rocks implies a necessary decoupling between the two modes of fracture during episodes of fast propagation. This may provide the mechanism for the observed slip partitioning. The geomorphology of the southern strand shows that fracture there is nearly pure mode II: “The strike-slip faulting

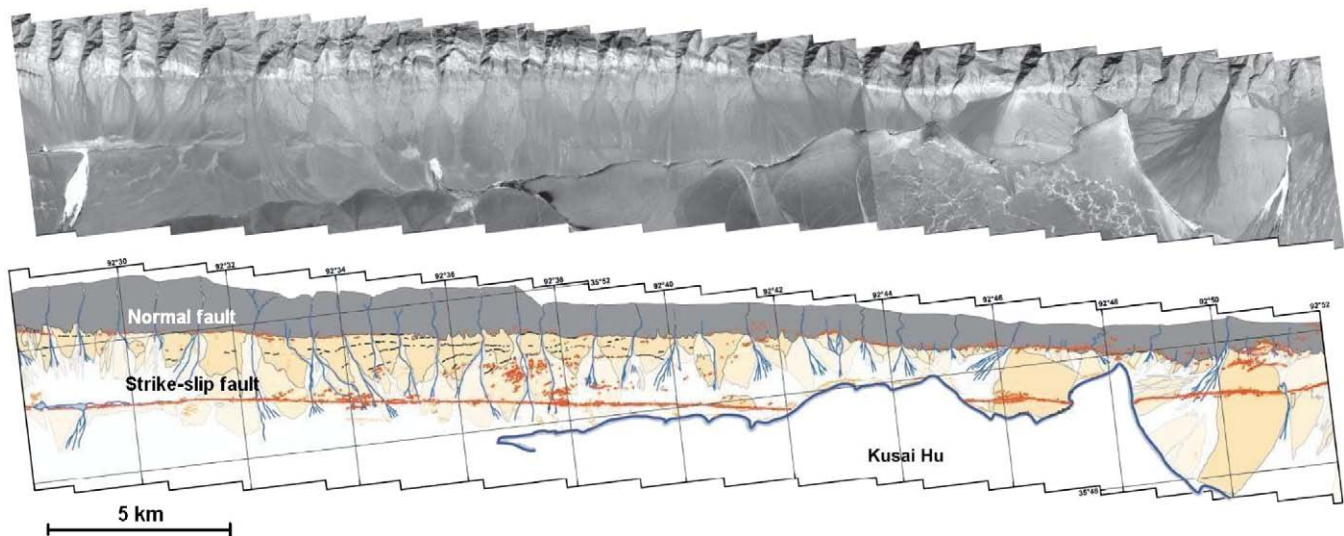


Fig. 9. (Top) Superposition of satellite (ICONOS) photographs showing part of the Kusai Hu segment of the Kunlun fault where slip partitioning occurred. (Bottom) Interpretation; Ruptures are shown by red lines. Modified from Klinger et al. (2005).

strand shows almost no evidence of significant vertical motion” (Xu et al., 2006). After running parallel to each other for about 70 km, the two strands merge again into a single fault zone, located at, or a few hundred meters south of, the mountain front. From this junction up to its termination about 165 km further east, the fault zone defines a single strand with little evidence of vertical motion.

3.5. Denali Fault earthquake

As mentioned earlier, there are relatively few details of the surface rupture along the inferred supershear section of the fault, the reason being that a large part of it occurs through glacier ice. Right-lateral offsets in this section average about 5 m, while measurements of vertical slip are typically around 50 cm (Haeussler et al., 2004).

4. Discussion

In all the documented observations of supershear ruptures, a striking common feature is the simple geometry of the fault. Its surface expression is always remarkably straight and continuous. Mechanically this seems to require and to imply that stress–strength conditions are relatively homogeneous along the fault. This is likely a key factor for allowing rupture to go supershear. This is consistent with two other sets of observations concerning supershear segments: the low level of high frequency radiation and the near-absence of aftershocks on the fault plane (Bouchon and Karabulut, 2008). The surprisingly low peak ground accelerations recorded near the Izmit (0.4 g) and Denali (0.36 g, Ellsworth et al., 2004) supershear segments are readily explained by the absence of strong heterogeneities which are the main source of high frequency seismic radiation (Madariaga, 1983).

Laboratory experiments and numerical simulations show that rupture speed is very sensitive to the presence of geometrical fault complexities such as bending, branching or step-overs and is often reduced by such encounters (Harris et al., 2002; Poliakov et al., 2002; Aochi and Madariaga, 2003; Rousseau and Rosakis, 2003, 2009; Bhat et al., 2004, 2007; Templeton et al., 2009). They also show that, under homogeneous pre-stress conditions, supershear rupture, when having the choice between dual branches, tends to favor a straight trajectory (Rousseau and Rosakis, 2009; Templeton et al., 2009). In particular, these authors show that for a fault branching geometry similar to the one existing in Kunlun at the end of the Kusai Hu segment (Fig. 5)

where the main Kunlun fault meets the Kunlun Pass fault, the straight trajectory is preferred. This is precisely what happened during the earthquake with rupture choosing the straight path—the Kunlun Pass fault—and leaving unbroken, east of the junction, the main Kunlun fault on which it had propagated until then. As told by Rousseau and Rosakis (2009) in the analysis of their experiment “the rupture velocity remains constant beyond the junction and moves past the secondary path as if it had been absent” and “the rupture crosses the junction without exhibiting any sign of having been disturbed and seemingly without having acquired knowledge of the existence of the incline”.

Another common feature of supershear observation is its association with remarkably pure Mode II rupture. Although this is consistent with theoretical predictions, it makes us wonder if sustained supershear rupture can develop in a mixed mode environment and if the mode decoupling it implies plays a role in slip partitioning.

5. Conclusion

Field investigations and satellite images show that faults which rupture at supershear speed during earthquakes have remarkably simple geometry. The linearity and continuity of supershear fault segments and the absence of significant segmentation features seem to require and to imply quite homogeneous strength–stress conditions along these segments. The homogeneity of friction along these faults is consistent with the lack of aftershocks and the low background seismicity of these segments. Sustained supershear rupture seems associated with remarkably pure Mode II rupture.

Acknowledgments

We thank Mustafa Aktar, Ares Rosakis, Nafi Toksöz, Bill Ellsworth, Raul Madariaga, Michel Dietrich, Anne-Marie Boullier, Cécile Cornou, Robert Guiguet, Pascal Bernard, Yann Klinger, Guillaume Daniel, David Baumont, Stefano Pucci, Elisa Tinti, Harsha Bhat, Hideo Aochi, Eric Dunham, Esen Arpat, Erdal Herece, Michel Campillo, Renata Dmowska, Jim Rice, Serdar Özalaybey, Ziyadin Çakir, Rolando Armijo, Bertrand Meyer, Jean-Bernard de Chabrier, Ozgun Konca, Jean-Philippe Avouac, Mustapha Meghraoui, Nikos Theodulidis, Peter Moczo, and Cécile Lasserre for their helpful insight and discussions.

References

- Aagaard, B.T., Heaton, T.H., 2004. Near-source ground motions from simulations of sustained intersonic and supersonic fault ruptures. *Bull. Seismol. Soc. Am.* 94, 2064–2078.
- Akyüz, H.S., Hartleb, R., Barka, A., Altunel, A., Sunal, G., Meyer, B., Armijo, R., 2002. Surface rupture and slip distribution of the 12 November 1999 Düzce earthquake (M 7.1), North Anatolian fault, Bolu, Turkey. *Bull. Seismol. Soc. Am.* 92, 61–66.
- Andrews, D.J., 1976. Rupture velocity of plane strain shear cracks. *J. Geophys. Res.* 81, 5679–5687.
- Aochi, H., Madariaga, R., 2003. The 1999 Izmit, Turkey, earthquake: Nonplanar fault structure, dynamic rupture process, and strong ground motion. *Bull. Seismol. Soc. Am.* 93, 1249–1266.
- Archuleta, R., 1984. A faulting model for the 1979 Imperial Valley earthquake. *J. Geophys. Res.* 89, 4559–4585.
- Arpat, E., Herece, E., Komut, T., Sentürk, K., 2001. 1999 Kocaeli and Düzce earthquake faults; their situations within the seismotectonic framework of the Marmara region. 54th Geol. Congress of Turkey, Proceedings CD, pp. 7–8.
- Awata, Y., Yoshioka, T., Emre, O., Duman, T.Y., Dogan, A., Tsukuda, E., Okamura, M., Matsuoka, H., Kuscu, I., 2003. Outline of the surface rupture of 1999 Izmit earthquake. Surface Rupture Associated with the 17 August 1999 Izmit Earthquake. In: Emre, et al. (Ed.), General Directorate of Mineral Research and Exploration. MTA, Ankara, pp. 41–55.
- Aydin, A., Kalafat, D., 2002. Surface ruptures of the 17 August and 12 November 1999 Izmit and Düzce earthquakes in northwestern Anatolia, Turkey: their tectonic and kinematic significance and the associated damage. *Bull. Seismol. Soc. Am.* 92, 95–106.
- Barka, A.A., Akyüz, H.S., Altunel, E., Sunal, G., Çakir, Z., Dikbas, A., Yerli, B., Armijo, R., Meyer, B., de Chabaliér, J.B., Rockwell, T., Dolan, J.R., Hartleb, R., Dawson, T., Christofferson, S., Tucker, A., Fumal, T., Langridge, R., Stenner, H., Lettis, W., Bachhuber, J., Page, W., 2002. The surface rupture and slip distribution of the 17 August 1999 Izmit earthquake (M 7.4) North Anatolian fault. *Bull. Seismol. Soc. Am.* 92, 43–60.
- Bhat, H.S., Dmowska, R., Rice, J.R., Kame, N., 2004. Dynamic slip transfer from the Denali to Totschunda faults, Alaska: testing theory for fault branching. *Bull. Seismol. Soc. Am.* 94, S202–S213.
- Bhat, H.S., Olives, M., Dmowska, R., Rice, J.R., 2007. Role of fault branches in earthquake rupture dynamics. *J. Geophys. Res.* 112, B11309. doi:10.1029/2007JB005027.
- Bouchon, M., Vallée, M., 2003. Observation of long supershear rupture during the M = 8.1 Kunlunshan earthquake. *Science* 301, 824–826.
- Bouchon, M., Karabulut, H., 2008. The aftershock signature of supershear earthquakes. *Science* 320, 1323–1325.
- Bouchon, M., Toksöz, M.N., Karabulut, H., Bouin, M.P., Dietrich, M., Aktar, M., Edie, M., 2000. Seismic imaging of the Izmit rupture inferred from the near-fault recordings. *Geophys. Res. Lett.* 27, 3013–3016.
- Bouchon, M., Bouin, M.P., Karabulut, H., Toksöz, M.N., Dietrich, M., Rosakis, A.J., 2001. How fast is rupture during an earthquake? New insights from the 1999 Turkey earthquakes. *Geophys. Res. Lett.* 28, 2723–2726.
- Bouchon, M., Toksöz, M.N., Karabulut, H., Bouin, M.P., Dietrich, M., Aktar, M., Edie, M., 2002. Space and time evolution of rupture and faulting during the 1999 Izmit (Turkey) earthquake. *Bull. Seismol. Soc. Am.* 92, 256–266.
- Bouin, M.P., Bouchon, M., Karabulut, H., Aktar, M., 2004. Rupture process of the 1999 November 12 Düzce (Turkey) earthquake deduced from strong motion and GPS measurements. *Geophys. J. Int.* 159, 207–211.
- Bürgmann, R., Ayhan, M.E., Fielding, E.J., Wright, T.J., McClusky, S., Aktung, B., Demir, C., Lenk, O., Türkez, A., 2002. Deformation during the 12 November 1999 Düzce, Turkey, earthquake, from GPS and InSAR data. *Bull. Seismol. Soc. Am.* 92, 161–171.
- Burridge, R., 1973. Admissible speeds for plane-strain self-similar shear cracks with friction but lacking cohesion. *Geophys. J. Roy. Astron. Soc.* 35, 439–455.
- Çakir, Z., de Chabaliér, J.B., Armijo, R., Meyer, B., Barka, A., Peltzer, G., 2003a. Coseismic and early post-seismic slip associated with the 1999 Izmit earthquake (Turkey) from SAR interferometry and tectonic field observations. *Geophys. J. Int.* 155, 93–110.
- Çakir, Z., Barka, A.A., de Chabaliér, J.B., Armijo, R., Meyer, B., 2003b. Kinematics of the November 12, 1999 (Mw = 7.2) Düzce earthquake deduced from SAR interferometry. *Turk. J. Earth Sci.* 12, 105–118.
- Das, S., Aki, K., 1977. A numerical study of two-dimensional spontaneous rupture propagation. *Geophys. J. Roy. Astron. Soc.* 50, 643–668.
- Dunham, E.M., Archuleta, R.J., 2004. Evidence for a supershear transient during the 2002 Denali fault earthquake. *Bull. Seismol. Soc. Am.* 94, S256–S268.
- Ellsworth, W.L., Celebi, M., 1999. Near field displacement time histories of the M 7.4 Kocaeli (Izmit), Turkey, earthquake of August 17, 1999. *Am. Geophys. Union, Fall Meeting Suppl.* 80, F648.
- Ellsworth, W.L., Celebi, M., Evans, J.R., Jensen, E.G., Kayen, R., Metz, M.C., Nyman, D.J., Roddick, J.W., Spudich, P., Stephens, C.D., 2004. Near-field ground motion of the 2002 Denali Fault, Alaska, earthquake recorded at Pum Station 10. *Earthquake Spectra* 20, 597–615.
- Emre, O., Erkal, T., Tchepalyga, A., Kazanci, N., Kececi, M., Ünay, E., 1998. Neogene–quaternary evolution of the eastern Marmara region, northwest Turkey. *Min. Res. Explor. Bull.* 120, 119–145.
- Feigl, K.L., Sarti, F., Vadon, H., McClusky, S., Ergintav, S., Durand, P., Bürgmann, R., Rigo, A., Massonnet, D., Reilinger, R., 2002. Estimating slip distribution for the Izmit mainshock from coseismic GPS, ERS-1, RADARSAT, and SPOT measurements. *Bull. Seismol. Soc. Am.* 92, 138–160.
- Frankel, A., 2004. Rupture process of the M 7.9 Denali fault, Alaska, earthquake: subevents, directivity, and scaling of high-frequency ground motion. *Bull. Seismol. Soc. Am.* 94, S234–S255.
- Freund, L.B., 1979. The mechanics of dynamic shear crack propagation. *J. Geophys. Res.* 84, 2199–2209.
- Fu, B., Lin, A., 2003. Spatial distribution of the surface rupture zone associated with the 2001 Ms 8.1 Central Kunlun earthquake, northern Tibet, revealed by satellite remote sensing data. *Int. J. Remote Sens.* 24, 2191–2198.
- Fu, B., Awata, Y., Du, J., Ninomiya, Y., He, W., 2005. Complex geometry and segmentation of the surface rupture associated with the 14 November 2001 great Kunlun earthquake, northern Tibet, China. *Tectonophysics* 407, 43–63.
- Haeussler, P.J., Schwartz, D.P., Dawson, T.E., Stenner, H.D., Lienkaemper, J.J., Sherrod, B., Cinti, F.R., Montone, P., Crow, P.A., Crone, A.J., Personius, S.F., 2004. Surface rupture and slip distribution of the Denali and Totschunda faults in the 3 November 2002 M 7.9 earthquake, Alaska. *Bull. Seismol. Soc. Am.* 94, S23–S52.
- Harris, R.A., Dolan, J.F., Hartleb, R., Day, S.M., 2002. The 1999 Izmit, Turkey, earthquake: a 3D dynamic stress transfer model of intraequake triggering. *Bull. Seismol. Soc. Am.* 92, 245–255.
- Hartleb, R.D., Dolan, J.F., Akyüz, H.S., Dawson, T.E., Tucker, A.Z., Yerli, B., Rockwell, T.K., Toraman, E., Çakir, Z., Dikbas, A., Altunel, E., 2002. Surface rupture and slip distribution along the Karadere segment of the 17 August 1999 Izmit and the western section of the 12 November 1999 Düzce, Turkey, earthquakes. *Bull. Seismol. Soc. Am.* 92, 67–78.
- Herece, E., Akay, E., 2003. Atlas of North Anatolian Fault (NAF). General Directorate of Mineral Research and Exploration, Special Publication series 2, Ankara, Turkey.
- King, G., Klinger, Y., Bowman, D., Tapponnier, P., 2005. Slip-partitioned surface breaks for the Mw 7.8 2001 Kokoxili earthquake, China. *Bull. Seismol. Soc. Am.* 95, 731–738.
- Klinger, Y., Xu, X., Tapponnier, P., van der Woerd, J., Lasserre, C., King, G., 2005. High-resolution satellite imagery mapping of the surface rupture and slip distribution of the Mw 7.8, 14 November 2001 Kokoxili earthquake, Kunlun fault, northern Tibet, China. *Bull. Seismol. Soc. Am.* 95, 1970–1987.
- Klinger, Y., Michel, R., King, G.C.P., 2006. Evidence for an earthquake barrier model from Mw 7.8 Kokoxili (Tibet) earthquake slip-distribution. *Earth Planet. Sci. Lett.* 242, 354–364.
- Konca, A.O., Leprince, S., Avouac, J.P., Helmberger, D.V. Rupture process of 2010, Mw = 7.1 Düzce earthquake from joint analysis of SPOT, GPS, InSAR, strong-motion and teleseismic data: a super-shear rupture with variable rupture velocity. *Bull. Seismol. Soc. Am.* 100, 267–288.
- Langridge, R.M., Stenner, H.D., Fumal, T.E., Christofferson, S.A., Rockwell, T.K., Hartleb, R.D., Bachhuber, J., Barka, A.A., 2002. Geometry, slip distribution, and kinematics of surface rupture on the Sakarya fault segment during the 17 August 1999 Izmit, Turkey, earthquake. *Bull. Seismol. Soc. Am.* 92, 107–125.
- Lasserre, C., Peltzer, G., Crampé, F., Klinger, Y., van der Woerd, J., Tapponnier, P., 2005. Coseismic deformation of the 2001 Mw = 7.8 Kokoxili earthquake in Tibet, measured by synthetic aperture radar interferometry. *J. Geophys. Res.* 110. doi:10.1029/2004JB003500.
- Lettis, W., Bachhuber, J., Witter, R., Brankman, C., Randolph, C.E., Barka, A., Page, W.D., Kaya, A., 2002. Influence of releasing step-overs on surface fault rupture and fault segmentation: examples from the 17 August 1999 Izmit earthquake on the North Anatolian fault, Turkey. *Bull. Seismol. Soc. Am.* 92, 19–42.
- Lin, A.B., Fu, B., Guo, J., Zeng, Q., Dang, G., He, W., Zhao, Y., 2002. Coseismic strike-slip and rupture length produced by the 2001 Ms 8.1 central Kunlun earthquake. *Science* 296, 2015–2017.
- Madariaga, R., 1983. High frequency radiation from dynamic earthquake fault models. *Ann. Geophys.* 1, 17–23.
- Michel, R., Avouac, J.P., 2002. Deformation due to the 17 August Izmit, Turkey, earthquake measured from SPOT images. *J. Geophys. Res.* 107. doi:10.1029/2000JB000102.
- Özalaybey, S., Aktar, M., Ergin, M., Karabulut, H., Bouchon, M., 2000. Aftershock studies following recent earthquakes in Turkey. XXVII General Assembly of the European Seismological Commission, Lisbon, Portugal.
- Poliakov, A.N.B., Dmowska, R., Rice, J.R., 2002. Dynamic shear rupture interaction with fault bends and off-axis secondary faulting. *J. Geophys. Res.* 107. doi:10.1029/2001JB000572.
- Pucci, S., 2006. The Düzce segment of the North Anatolian Fault Zone (Turkey): Understanding its seismogenic behavior through earthquake geology, tectonic geomorphology and paleoseismology. Ph.D. Thesis, Università degli Studi di Perugia, Perugia, Italy.
- Pucci, S., Pantosti, D., Barchi, M.R., Palyvos, N., 2006. Evolution and complexity of the seismogenic Düzce fault zone (Turkey) depicted by coseismic ruptures, plio-quaternary structural pattern and geomorphology. *Earth Planet. Sci. Lett.*
- Reilinger, R.E., Ergintav, S., Bürgmann, R., McClusky, S., Lenk, O., Barka, A.A., Gürkan, O., Hearn, E.H., Feigl, K.L., Cakmak, R., Aktug, B., Ozener, H., Toksöz, M.N., 2000. Coseismic and postseismic fault slip for the 17 August 1999 M = 7.5, Izmit, Turkey earthquake. *Science* 289, 1519–1524.
- Robinson, D.P., Brough, C., Das, S., 2006. The Mw 7.8 2001 Kunlunshan earthquake: extreme rupture speed variability and effect of fault geometry. *J. Geophys. Res.* 111. doi:10.1029/2005JB004137.
- Rosakis, A.J., Samudrala, O., Coker, D., 1999. Cracks faster than the shear wave speed. *Science* 284, 1337–1340.
- Rousseau, C.E., Rosakis, A.J., 2003. On the influence of fault bends on the growth of sub-Rayleigh and intersonic dynamic shear ruptures. *J. Geophys. Res.* 108. doi:10.1029/2002JB002310.
- Rousseau, C.E., Rosakis, A.J., 2009. Dynamic path selection along branched faults: experiments involving sub-Rayleigh and supershear ruptures. *J. Geophys. Res.* 114, B08303. doi:10.1029/2008JB006173.

- Sharp, R.V., Lienkaemper, J.J., Bonilla, M.G., Burke, D.B., Fox, B.F., Herd, D.H., Miller, D.M., Morton, D.M., Ponti, D.J., Rymer, M.J., Tinsley, J.C., Yount, J.C., Kahle, J.E., Hart, E.W., Sieh, K.E., 1982. Surface faulting in the central Imperial valley. The Imperial Valley, California, earthquake of October 15, 1979, U.S. Prof. Paper 1254, pp. 119–143.
- Spudich, P., Cranswick, E., 1984. Direct observation of rupture propagation during the 1979 Imperial Valley earthquake using a short baseline accelerometer array. *Bull. Seismol. Soc. Am.* 74, 2083–2114.
- Templeton, E.L., Baudet, A., Bhat, H.S., Dmowska, R., Rice, J.R., Rosakis, A.J., Rousseau, C.E., 2009. Finite element simulations of dynamic shear rupture experiments and dynamic path selection along kinked and branched faults. *J. Geophys. Res.*, 114, B08304, doi:10.1029/2008JB006174.
- Vallée, M., Landès, M., Shapiro, N.M., Klinger, Y., 2008. The 14 November 2001 Kokoxili (Tibet) earthquake: High frequency seismic radiation originating from the transition between sub-Rayleigh and supershear rupture velocity regimes. *J. Geophys. Res.* 113, B07305. doi:10.1029/2007JB005520.
- van der Woerd, J., Meriaux, A.S., Klinger, Y., Ryerson, F.J., Gaudemer, Y., Tapponnier, P., 2002. The 14 November 2001, Mw=7.8 Kokoxili earthquake in northern Tibet. *Seismol. Res. Lett.* 73, 125–135.
- Walker, K.T., Shearer, P.M., 2009. Illuminating the near-sonic rupture velocities of the intracontinental Kokoxili Mw 7.8 and Denali Fault Mw 7.9 strike-slip earthquakes with global P-wave back projection imaging. *J. Geophys. Res.* 114, B02304. doi:10.1029/2008JB005738.
- Wen, Y.Y., Ma, K.F., Song, T.R.A., Mooney, W.D., 2009. Validation of the rupture properties of the 2001 Kunlun, China (Ms=8.1), earthquake from seismological and geological observations. *Geophys. J. Int.* 177, 555–570.
- Xia, K., Rosakis, A.J., Kanamori, H., 2004. Laboratory earthquakes: the sub-Rayleigh-to-supershear transition. *Science* 303, 1859–1861.
- Xu, X., Chen, W., Ma, W., Yu, G., Chen, G., 2003. Surface rupture of the Kunlunshan earthquake (Ms8.1), northern Tibetan plateau, China. *Seismol. Res. Lett.* 73, 884–892.
- Xu, X., Yu, G., Klinger, Y., Tapponnier, P., van der Woerd, J., 2006. Reevaluation of surface rupture parameters and faulting segmentation of the 2001 Kunlunshan earthquake (Mw 7.8), northern Tibetan Plateau, China. *J. Geophys. Res.* doi:10.1029/2004JB003488